applied sciences

MDPI

Article

Effect of Alkali Concentration on the Activation of Carbonate-High Illite Clay

Angela D'Elia [1], Daniela Pinto [1,*], Giacomo Eramo [1], Rocco Laviano [1], Angel Palomo [2] and Ana Fernández-Jiménez [2,*]

[1] Dipartimento di Scienze della Terra e Geoambientali, Università degli Studi di Bari Aldo Moro, 70121 Bari, Italy; angela.delia@uniba.it (A.D.); giacomo.eramo@uniba.it (G.E.); rocco.laviano@uniba.it (R.L.)
[2] Instituto Eduardo Torroja (CSIC), 28033 Madrid, Spain; palomo@ietcc.csic.es
* Correspondence: daniela.pinto@uniba.it (D.P.); anafj@ietcc.csic.es (A.F.-J.)

Received: 25 February 2020; Accepted: 16 March 2020; Published: 25 March 2020

Abstract: The present study explores the effect of activating solution concentration (4, 6 and 8 M NaOH) on mechanically and thermally pre-treated carbonate-high illite clay (LCR). Pastes were prepared with an alkaline solution/clay (S/B) ratio of 0.55, which were cured at room temperature and relative humidity > 90% in a climatic chamber. At two and 28 days, compressive mechanical strength was determined, and the reaction products were characterised by X-ray Powder Diffraction analysis (XRPD), Fourier-transform infrared spectroscopy (FTIR) and Scanning Electron Microscopy - Energy Dispersive X-ray spectroscopy (SEM/EDX). Results obtained showed that the presence of reactive calcium in the starting clay induces co-precipitation of a mix of gels: An aluminium-enriched C-S-H gel (C-A-S-H) and a N-A-S-H gel, in which sodium is partially replaced by calcium (N,C)-A-S-H. Pastes prepared with higher (6 or 8 M) activator concentrations exhibit a more compact matrix than the ones prepared with 4 M NaOH. The findings show that the use of a 6 M NaOH solution yields a binder with two days compressive strength >20 MPa and 28 days strength of over 30 MPa.

Keywords: carbonate-high illite clay; alkali activation; NaOH; activator concentration

1. Introduction

Alkali-activated materials (AAMs) are binders obtained when aluminosilicate materials ("precursors") react chemically with an alkaline activator (normally an alkaline hydroxide or alkaline silicate solution) [1–6]. As materials with a low environmental impact, AAMs are attracting considerable research as cements for the future, along with limestone calcined clay (LC3) [7,8] and belite–ye'elimite–ferrite (BYF) cements [9,10].

One of the major technological challenges to be faced in alkaline activation is to find precursors that are both widely available and technically suitable. The aluminosilicates most commonly used include burnt kaolinite clay and industrial by-products such as fly ash (FA) and ground granulated blast furnace slag (GGBFS) [11–13]. Output of FA and GGBFS is very high at this time and both will continue to be readily available during the twenty-first century. Nonetheless, the environmental challenges facing humanity herald a decline in future production, and the universal geographic availability for industrial scale AAM manufacture is not guaranteed. Pure kaolinite clay (metakaolin) deposits, in turn, are characterised by limited market availability and competition from other industries (paper, fired clay ceramics), which raise the cost of this raw material. Moreover, metakaolin-based AAMs are subject to workability [14] and drying shrinkage [15] problems.

In contrast, clay minerals, outside of very pure kaolinite, constitute an abundant source of aluminosilicates, available worldwide. Studies carried out in recent years on ways to enhance the reactivity of "low purity" clay minerals, with a view to AAM [14,16] and LC3 [7,8] cement manufacture,

have shown that their mineralogy (crystallinity), texture, and particle size [17–21] affect its reactivity. As a rule, lower crystallinity, greater surface amorphism and smaller particle size lead to higher initial reactivity in precursors and hence to binders with greater initial mechanical strength. Most of the studies published described clays with a low calcium oxide content such as kaolinite [6,22–24], illite [25–27], bentonite [28,29] or even sedimentary [5,20] materials.

The main post-alkali-activation reaction product in precursors with a low CaO content (<10%) is a three-dimensional alkaline aluminosilicate hydrate gel (Na_2O-Al_2O_3-SiO_2-H_2O) commonly named as, N-A-S-H. Conversely, if the CaO content in the precursor is fairly high (30% to 40%, such as in blast furnace slag), the main reaction product is a two-dimensional calcium aluminosilicate hydrate gel (CaO-Al_2O_3-SiO_2-H_2O), commonly named as, C-A-S-H [11,12]. These two gels differ both chemically and structurally from the calcium silicate hydrate (CaO-SiO_2-H_2O), commonly named as C-S-H, that precipitates as the main hydration product in ordinary Portland cement (OPC) [7].

Activator CaO content and pH, which also play a significant role in the chemical composition and structure of the cementitious gels forming in AAMs, constitute a promising field of research at this time [11,12]. Many studies have shown [30,31] that mixing a precursor with moderate (20% to 30%) amounts of calcium in 4 to 5 M caustic solutions favours the solution/precipitation of a C-A-S-H gel at ambient temperature. Higher alkalinity may raise the degree of reaction and Si and Al (although not Ca) solubility, favouring the precipitation of a N-A-S-H gel or a mix of N-A-S-H/C-A-S-H gels that may interact over time [32] to make (N,C)-A-S-H (calcium-bearing N-A-S-H) gel or C-(N)-A-S-H (sodium bearing C-A-S-H) gel. The composition and structure of the aforementioned gel/mix of gels and the parameters affecting their nature and stability (pH, temperature, moisture ...) are studied in the so-called "hybrid alkaline cements" obtained in the alkaline activation of blends bearing approximately 20 wt.% of CaO, SiO_2 and Al_2O_3 [33,34].

Against that backdrop, the present study forms part of broader research that explores the potential of carbonate-bearing (~30% CaO) illite clay in alkaline cement formulation. In earlier experiments [21] focused on optimising milling, temperature and thermal treatment to raise clay reactivity, the authors observed that intense clay grinding lowered clay mineral decomposition temperatures. Milling for 15 min in a high energy mixer mill followed by heating at 700 °C for 1 h was found to be the most effective pre-activation treatment for calcium carbonate-high illite clays for the intents and purposes of geopolymer manufacture.

The present study explores the effect of activating solution concentration (4, 6 and 8 M NaOH) on carbonate-bearing, mechanically and thermally pre-treated illite clays. More specifically, the material used was a carbonate-high illite clay largely occurring in southern Italy (Apulia and Basilicata regions), which may constitute an innovative, widely available and suitable precursor for alkaline cement production. The findings can be extrapolated to other carbonate-bearing clays as well as to other possible precursors with a similar composition. The authors note that this study also affords the opportunity for in-depth research into the role of calcium and the degree of alkalinity on alkaline activation.

2. Materials and Methods

The material used in this study was a carbonate-high illite clay (LCR) mined in the region of Apulia, Lucera, FG, Italy. Based on earlier findings [21], this clay was pre-treated mechanically (15 min at 1800 rpm in a Retsch MM 400 mixer mill) and thermally (700 °C for 1 h) to yield a clay here labelled MA157. Table 1 gives the chemical compositions of the original and pre-treated clays as found on a Panalytical AXIOS-Advanced XRF spectrometer fitted with an X SST-mAX (Rh anode) X-ray source. The table also lists the XRD (Rietveld method)-determined mineralogical composition for the clays [21].

Table 1. Bulk chemical composition and mineralogical content of the original untreated clay and pre-treated MA157.

Chemical Composition (wt%) XRF			Mineralogical Composition (wt%, 3σ)		
	Untreated Clay	**MA157** [1]		**Untreated Clay**	**MA157** [1]
SiO_2	35.67	43.05	**Quartz**	16.3 (0.7)	20.6 (1.4)
Al_2O_3	11.47	13.14	**Calcite**	31.2 (1.3)	5.4 (1.1)
CaO	21.15	29.97	**Illite/Muscovite**	3.8 (0.5)	3.5 (1.0)
K_2O	1.73	2.28	***R*0 illite(0.3)/smectite mixed layers** [2]	24.5 (2.9)	-
Na_2O	0.34	0.36	**Kaolinite**	5.9 (1.0)	
Fe_2O_3	6.67	9.34	**K-feldspar**	4.2 (1.0)	10.6 (1.7)
MgO	1.91	2.22	**Albite**	3.2 (0.5)	3.4 (0.8)
MnO	0.15	0.21	**Goethite**	1.7 (0.2)	-
TiO_2	0.53	0.73	**Hematite**	-	2.8 (0.5)
P_2O_5	0.07	0.09	**Dolomite**	1.0 (0.2)	-
LoI	20.32	0.61	**Chlorite**	1.0 (0.3)	-
			Amorphous matter	7.1 (6.3)	53.9 (3.6)
			Tot C.M.	35.2 (3.7)	3.5 (1.0)

[1] Clay ground in a mixer mill and subsequently heated to 700 °C; [2] illite/smectite interstratifications of *R*0 (Reichweite) ordering type and with composition of 30 mol% illite and 70 mol% smectite according to the nomenclature from Moore and Reynolds [35]. Tot C. M. stands for total clay minerals.

Figure 1 shows the particle size distribution for clay MA157 dispersed via ultrasound in a DOLAPIX CE64 1/100 ethanol and dispersion medium, as determined on a SYMPATEC laser sizer with a measuring range of 0.05 to 875 μm.

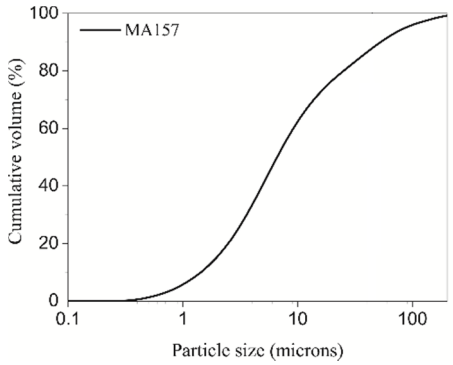

Figure 1. MA157 particle size distribution.

MA157 clay pastes were prepared with 4, 6 and 8 M solutions of NaOH at an alkaline solution/clay (S/B) ratio of 0.55, previously found to be the most suitable to ensure good paste workability. The pastes were subsequently poured into prismatic ($1 \times 1 \times 6$ cm^3) moulds and cured at ambient temperature and relative humidity > 90% in a climate chamber. They were removed from the moulds 20 h later and stored in the climate chamber until the 2 and 28 days test ages, when six samples at each age were tested for compressive strength on an IBERTEST® test frame (six specimens per test age and material were tested).

The reaction products were analysed by X-ray Powder Diffraction analysis (XRPD) with a Bruker AXS D8 Advance Cu-Kα radiation diffractometer operating at 30 mA and 40 kV across a 2θ range of 5° to 60° and scanning at 0.0197° (2θ) steps. They were likewise characterised Fourier-transform infrared spectroscopy (FTIR), on KBr pellets (1 mg of sample in 200 mg of KBr) with a Nicolet Thermo FTIR spectrometer, recording 64 scans per sample at 4000 to 400 cm^{-1}. Lastly, the products were analysed along the sputter-coated fracture surfaces of the samples under Scanning Electron Microscopy - Energy Dispersive X-ray spectroscopy (SEM/EDX) a JEOL JSM 5400 SEM equipment fitted with an Oxford

Link-ISIS-EDX spectrometer, collecting the images with secondary electrons (SE) at a working distance of 15 mm and a 20 kV accelerating voltage. The EDX (point) analyses were conducted with a 20 μm beam, also at a 20 kV accelerating voltage and a working distance of 15 mm. Acquisition time was 30 s per point analysis.

3. Results and Discussion

3.1. Mechanical Strength

Figure 2 shows the two and 28 days compressive strengths for the MA157 pastes prepared with 4, 6 and 8 M NaOH solutions. In the two days materials, the highest strength, at >25 MPa, was recorded for the pastes prepared with 6 M NaOH. The 28 days pastes exhibited strength of 32 MPa at 4 M NaOH, 33 MPa at 6 M NaOH and 36 MPa at 8 M NaOH. The increase in mechanical strength with time was attributed to the greater degree of reaction, although strength was also observed to depend on reaction product chemical, mineralogical and microstructural composition, as discussed in a later section.

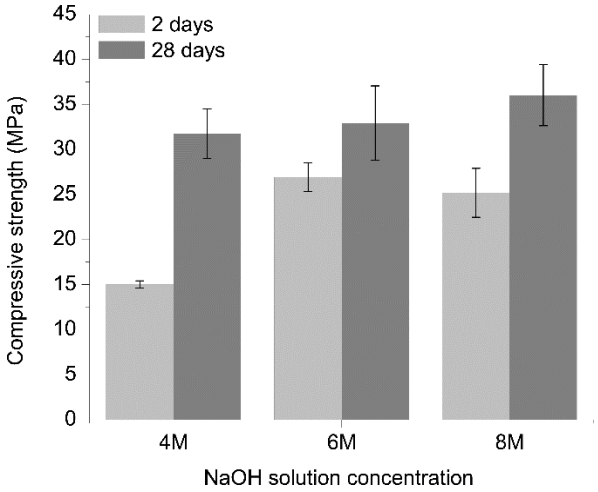

Figure 2. Two and 28 days compressive strength in 4, 6 and 8 M NaOH-activated pastes (six specimens per test age and material were tested).

The compressive strength values recorded here were higher than reported by other authors, who worked with thermally treated alkali-activated illite/smectite clay with CaO contents of <5%. Buchwald et al. [25] found compressive strength values of around 13 MPa with 6 M NaOH, (solution/solid ratio = 0.41, curing 20 h at 20 °C in sealed moulds avoiding drying out, after demoulding; seven days at 60 °C in 100% relative humidity (RH), 3 h at 80 °C in 100% RH and drying over 24 h at 40 °C). Essaidi et al. [26], using a potassium silicate solution, observed strength of 25 MPa (initial curing in an opened polystyrene sealed mould, 48 h at 70 °C, subsequently, the mould was closed into oven at 70 °C for 2 h; after demoulding ambient air (25 °C, 40% RH) during 21 days). Seiffarth et al. [19] obtained values of <10 MPa with sodium silicate molar ratio of SiO_2/Na_2O = 0.31 (initial curing in wet conditions, seven days, 25 °C and 85% RH, followed by curing in dry conditions: Three days, 40 °C, 55% RH).

The higher strength values found in this study were attributed to the high degree of clay reaction, the outcome of the initial mechanical-thermal treatment. As the benefits of that treatment, which induces phyllosilicate amorphism and carbonate decomposition, were described in detail in an earlier paper [21], they are not addressed hereunder. Another factor deemed to have contributed significantly to the good initial mechanical performance of this alkali-activated, ambient temperature-cured clay, was the presence of a fairly high (~30%) proportion of calcium. Like silicon and aluminium, calcium solubility is heavily dependent upon system alkalinity. Given that solution alkalinity played a substantial role in these complex systems (~43% SiO_2, 13% Al_2O_3 and 30% CaO, see Table 1), it was defined as the primary object of the present study.

3.2. Reaction Products

The XRD patterns for clay MA157 and the three (4, 6 and 8 M) pastes are reproduced in Figure 3. The precursor exhibited a significant amorphous component at 2θ values of 20° to 40°. The crystalline phases detected in MA157 included quartz, calcite, illite/muscovite, K-feldspar (orthoclase, albite and anorthite) and plagioclase. With the exception of calcite, the intensity of these diffraction lines barely varied after alkaline activation, an indication that the respective phases were inert. The patterns for all the pastes showed a slight shift in the hump located in the precursor at 2θ = 20° to 40° to around 2θ = 30° to 40° (the hump is a characteristic of amorphous and/or glassy phases) denoting a reaction between the amorphous phases in the clay and the formation of new, low structural order phases, primarily cementitious gels [4]. The lines attributed to the presence of calcite were more intense in the paste activated with 4 M NaOH. Although less calcite was formed at higher alkali concentrations (6 and 8 M), sodium carbonates or calcites such as natron ($Na_2CO_3{\cdot}10H_2O$ (PDF # 00-015-0800)) and gaylussite ($Na_2Ca(CO_3)_2{\cdot}5H_2O$) (PDF # 00-021-0343)) were detected on their diffractograms.

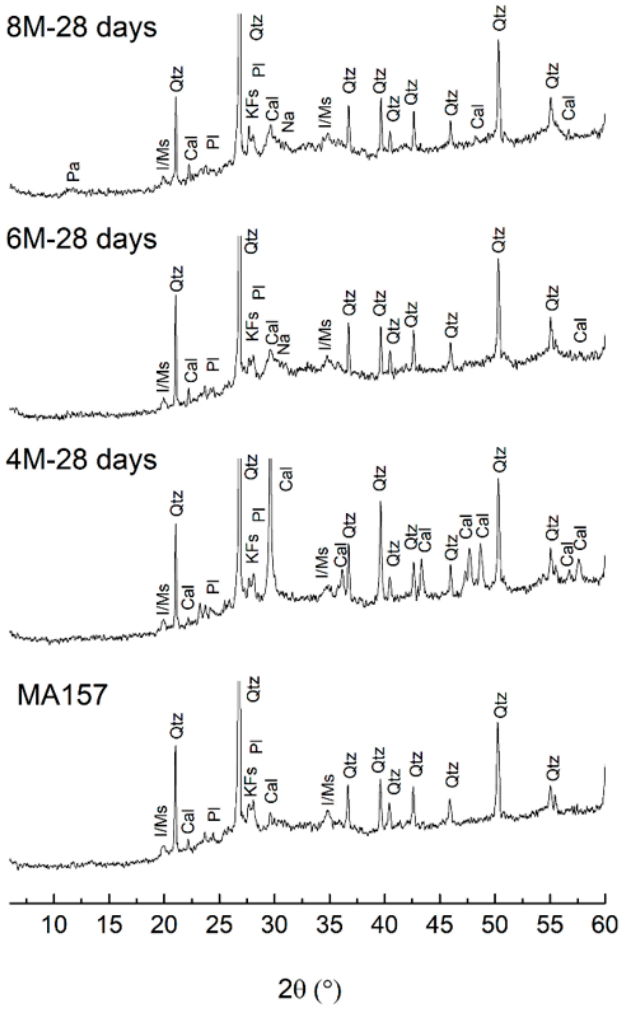

Figure 3. XRD patterns for anhydrous MA157 clay and 28 days, 4, 6 and 8 M NaOH-activated pastes Legend: I/Ms = illite/muscovite; Qtz = quartz; Pl = plagioclase, Kfs = K-feldspar, Cal = calcite; Na = natron; Pa = para-alumohydrocalcite/hemicarboaluminate.

Unlike other alkali-activated binders made with dehydroxylated clay as precursors [25–27], the pastes prepared here contained no zeolite crystals. That absence was attributed in part to the fairly low (13.4%) aluminium content in MA157 and/or to ambient temperature curing which would lower Al solubility. A number of authors have reported that zeolite formation as a secondary product in alkaline

cements depends on both the reactive aluminium content and the synthesis parameters, primarily activator type and concentration [11,12,36], and curing conditions (time, temperature, humidity) [4,37].

A small hump was observed at 2θ = 10° to 11°, possibly associated with the formation of para-alumohydrocalcite ($CaAl_2(CO_3)_2(OH)_4{\cdot}6H_2O$ (PDF# 00-030-0222)), a hydrotalcite group mineral, or hemicarboaluminate ($Ca_4Al_2O_7CO_2{\cdot}11H_2O$ (PDF# 00-036-0377)). These phases are often present as secondary reaction products in calcium-high alkaline cements such as alkali-activated blast furnace slag [38] or limestone-metakaolin blends [39].

The FTIR spectra for clay MA157 and the two and 28 days pastes are reproduced in Figure 4. The spectrum for the starting material exhibited a wide band at approximately 1079 to 1086 cm^{-1}, associated with the asymmetric stretching vibrations generated by the Si-O-T (T = Si, Al) bonds possibly present in the amorphous component of the material [40]. It also contained vibration bands characteristics of quartz at 1084, 796, 694 and 463 cm^{-1} [41], a low intensity band at 1438 cm^{-1} attributed to the presence of calcium carbonate and another at 1635 cm^{-1} to the bending vibrations generated by the OH groups in water [41].

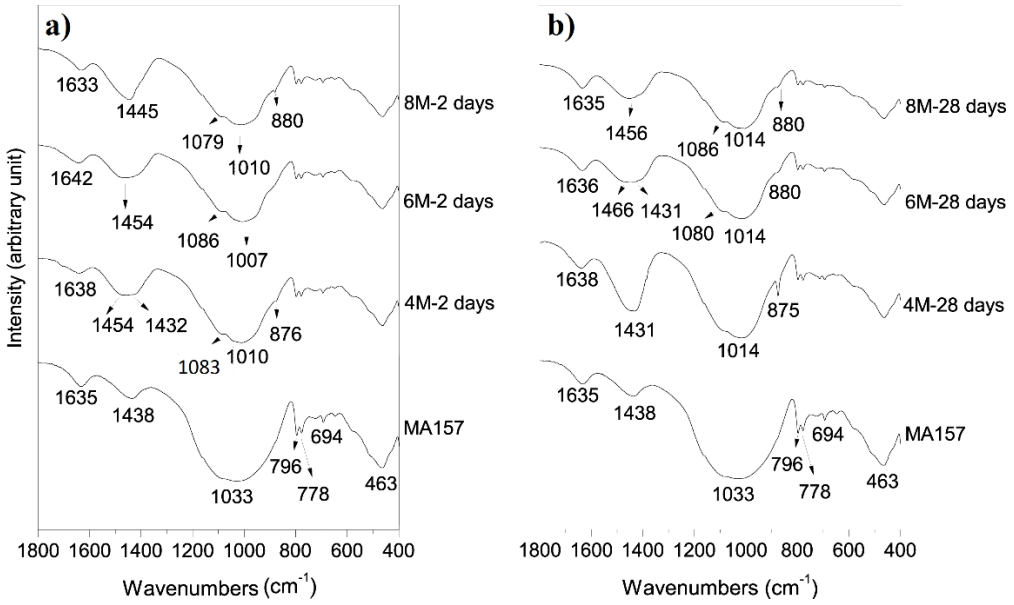

Figure 4. FTIR spectra for anhydrous MA157 clay and (**a**) two days and (**b**) 28 days pastes alkali-activated with 4, 6 and 8 M NaOH.

The Si-O-T (T = Si, Al) stretching band in the pastes was shifted to lower frequencies and its signal grew narrower at longer reaction times. That band appeared at 1010 cm^{-1} in the two days and at 1014 cm^{-1} in the 28 days pastes. Further to the literature [4,9,40,41], these variations stem from the initial alkaline-mediated dissolution of the amorphous/reactive component in the clay and the ensuing precipitation of a cementitious gel with a fairly high aluminium content (intermediate reaction product, band at 1010 cm^{-1}). The formation of that intermediate product would be explained by the synchronised dissolution of the aluminium and silicon ions in the alkaline medium in the initial stages. As the aluminium content was fairly low, upon its depletion the silicon would continue to react, affording the gel a higher proportion of silicon and shifting the FTIR band to higher values (1014 cm^{-1}).

The carbonate band on the spectra for the activated pastes were both shifted to slightly higher or lower wave numbers (1400 to 1500 cm^{-1}) and somewhat more intense. A shoulder appearing at 875 cm^{-1} confirmed the formation of the carbonates detected with XRD in the alkali-activated MA157 clay pastes. More specifically, vibration bands characteristic of calcite were observed at approximately 1432, 876 and 710 cm^{-1} [42,43] in the 4, 6 and 8 M NaOH-activated pastes, whereas the signal at approximately 1450 cm^{-1} might be attributed to sodium carbonate [43]. The bands associated with

the presence of calcite were most intense on the spectrum for the 28 days sample activated with 4 M NaOH (Figure 4b), a finding consistent with the XPRD results (Figure 3).

Figure 5 depicts the two days and Figure 6 the 28 days micrographs for the 4, 6 and 8 M NaOH-activated pastes. A cementitious matrix consisting primarily in Si, Al and Ca was identified in all. The EDX analyses showed that the proportions of these elements, calcium in particular, varied depending on activator concentration and curing time. That finding was associated with the possible formation of a mix of (N,C)-A-S-H/N-(C)-A-S-H gels. The formation of that mix of gels and the high early mechanical strength at ambient temperature were primarily the outcome of the presence of calcium in these dehydroxylated clays [32,44,45]. Activator alkalinity also affected the type and proportion of the C-A-S-H (Al-enriched C-S-H) and/or (N,C)-A-S-H (calcium-bearing N-A-S-H) gels formed, as well as the amount and composition of the secondary reaction products (such as carbonates or AFm phases) (Figure 3).

As a rule the microstructure of the 2 days, 4 M NaOH-activated paste was less uniform than in the other materials (Figure 5a). The phases in the form of Ca-high plates in the Si, Al and Ca-containing cementitious matrix suggested the formation of an Al-tobermorite-like compound. In the 28 days 4 M-activated paste, the matrix was less compact and more granular (Figure 6a). That observation was associated with the significant carbonation in the 4 M NaOH-activated pastes (as revealed by the XRD and FTIR results) that apparently induced decalcification of the C-A-S-H-like cementitious gel. The EDX analyses denoted a lower calcium content in the 28 days than in the two days gels. Similar decalcification was described by Puertas et al. [46] in a study of C-A-S-H gel carbonation in a study of the alkaline activation of blast furnace slag.

At the two higher alkalinities, the microstructure was more uniform and compact. Nonetheless, the excess sodium from the higher concentration of the activating solution (especially in the 8 M NaOH-activated samples) induced calcium and sodium carbonate salt precipitation, as confirmed by the EDX analyses (Figure 5(c2)). The resulting calcite crystals were primarily located in, and filling, the matrix pores.

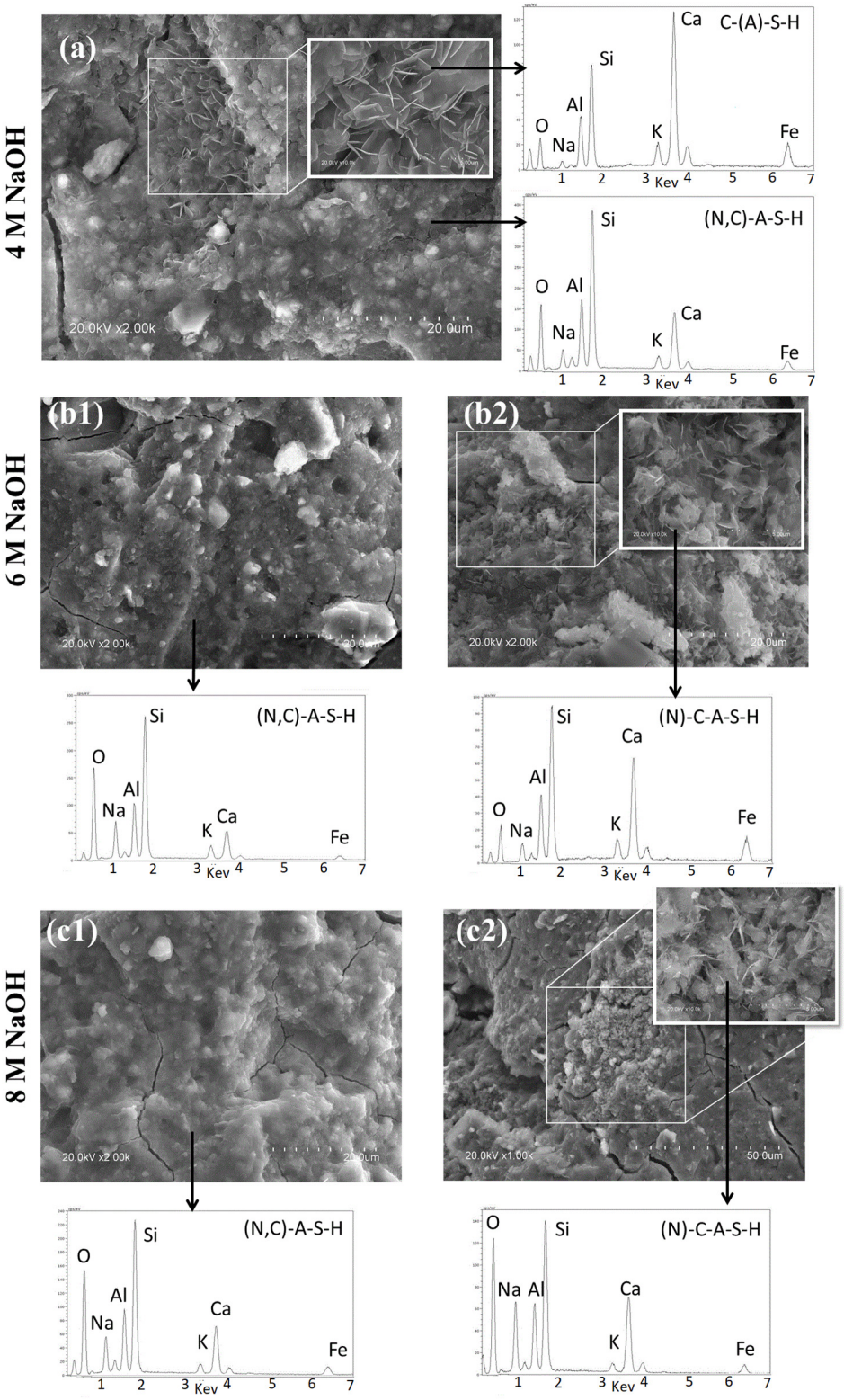

Figure 5. Two day SEM micrographs and EDX spectra for (**a**) 4 M, (**b**) 6 M (**b1**,**b2**) and (**c**) 8 M (**c1**,**c2**) NaOH-activated pastes.

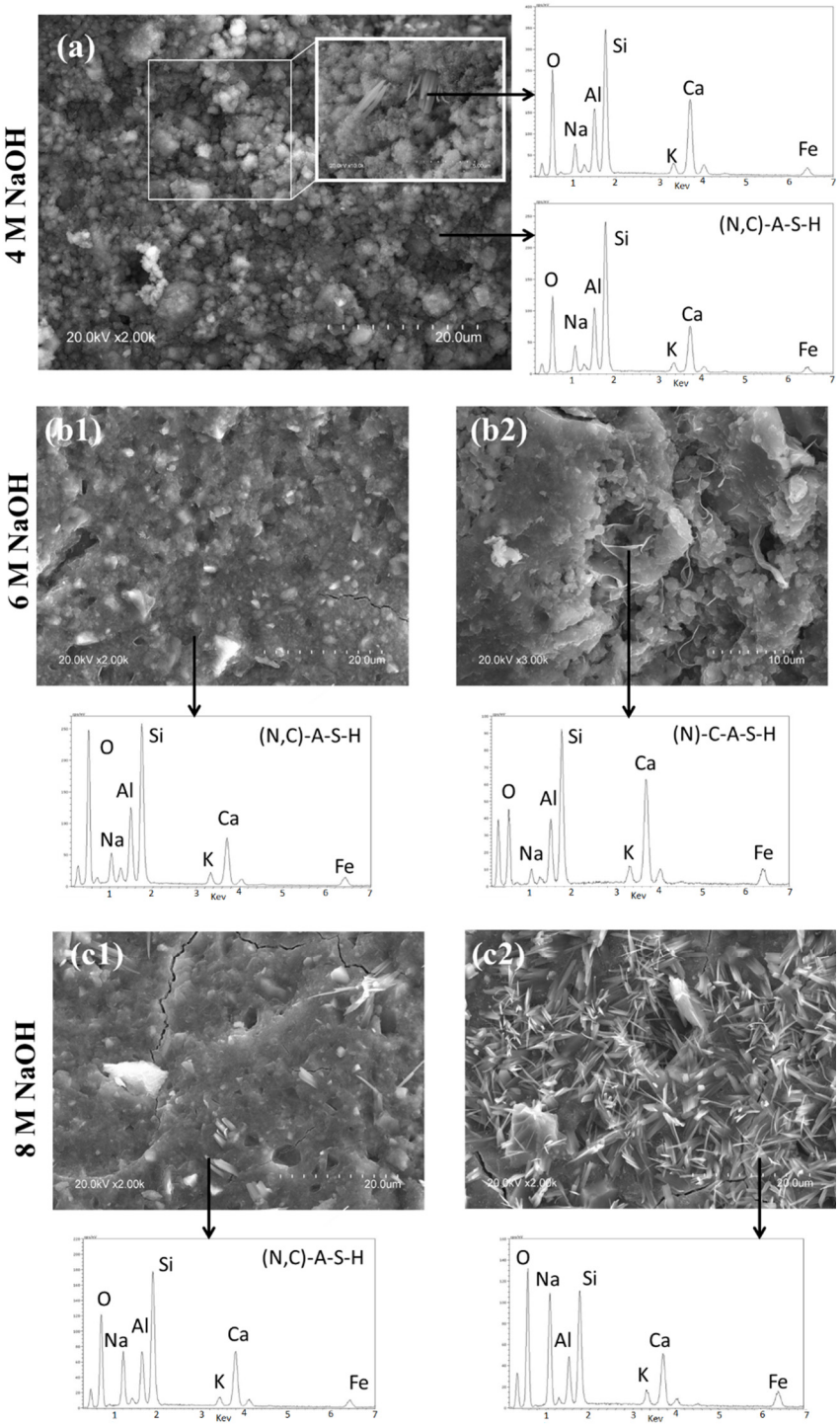

Figure 6. Twenty-eight day SEM micrographs and EDX spectra for (**a**) 4 M, (**b**) 6 M (**b1**,**b2**) and (**c**) 8 M (**c1**,**c2**) NaOH-activated pastes.

The EDX-determined variability in gel composition was graphed on CaO-Al_2O_3-SiO_2 and Na_2O-Al_2O_3-SiO_2 ternary diagrams (Figure 7) to study the effect of activator concentration on the type or types of gels formed. The findings showed that in all the cases studied, the alkaline activation of carbonate-high clays with NaOH solutions entailed the co-precipitation of a mix of C-A-S-H- and (N,C)-A-S-H-like gels, which had a higher SiO_2 and a lower Al_2O_3 content (i.e., a higher SiO_2/Al_2O_3 ratio) than other gels described in the literature [32]. Chemically speaking, these gels are more like the ones forming in blast furnace slag [47,48] than in dehydroxylated kaolinite alkaline activation [14,27].

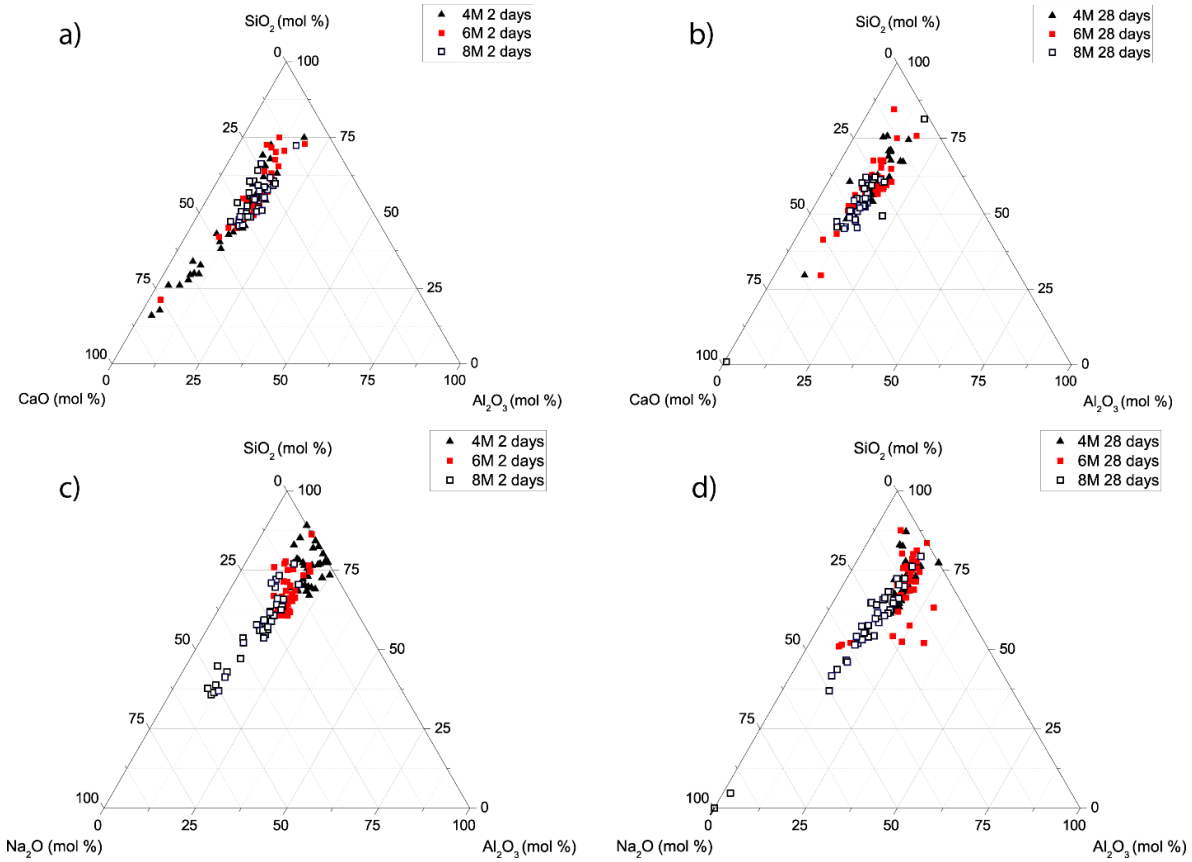

Figure 7. EDX data for the two and 28 days, 4, 6 and 8 M NaOH-activated pastes graphed on (**a**,**b**) $CaO-Al_2O_3-SiO_2$; and (**c**,**d**) $Na_2O-Al_2O_3-SiO_2$ ternary diagrams.

When the activator was 4 M NaOH and the time two days, although scattered, calcium clearly prevailed. The points with >60% CaO were associated with the Ca-high, plate-like particles visible in Figure 5a. Given their chemical composition and shape, those phases would appear to be consistent with an aluminium-enriched C-S-H such as Al-tobermorite [32,49,50].

The clusters observed on the micrographs for the two days, 6 and 8 M NaOH-activated pastes (Figure 7a) were characterised by a non-uniform distribution of CaO, ranging from 25% to 60% and associated with the precipitation of a mix of an Al-enriched C-S-H gel (C-A-S-H) and a calcium-bearing N-A-S-H gel (N,C)-A-S-H). With time, higher activator alkalinity (especially visible for 8 M NaOH) induced (N,C)-A-S-H gel evolution toward a C-A-S-H gel. Earlier studies [32] showed that N-A-S-H gel may persist at lower pH (<12), whereas in the presence of calcium, ionic exchange prompts the formation of (N,C)-A-S-H gel, in which calcium may be taken up until it ultimately replaces all the sodium in the cementitious gel's three-dimensional structure.

The 28 days, 8 M NaOH-activated MA157 paste exhibited a chemical composition primarily attributable to a C-A-S-H gel, although at 0.24 ± 0.07 the Al_2O_3/SiO_2 molar ratio was lower than the 0.3 to 0.5 range normally observed for such gels [32]. That was due the higher SiO_2 than Al_2O_3 content in the starting clay. In contrast, the matrix for that same paste exhibited a CaO/SiO_2 molar ratio of 0.64 ± 0.17, consistent with the range suggested in the literature ($0.6 < CaO/SiO_2 < 1$) for C-A-S-H gels [32,48]. The chemical composition of the 28 days, 6 M NaOH-activated pastes also moved toward higher CaO contents in the $CaO-Al_2O_3-SiO_2$ ternary diagrams (Figure 7b) than the two days pastes (Figure 7a).

In contrast, the matrices for the 28 days, 4 M NaOH-activated pastes were characterised by a lower CaO/SiO_2 ratio than the two days materials (Figure 7a,b) and a higher Na_2O uptake in the gel as the reaction progressed (Figure 7d). Those findings may be attributed to the higher carbonation observed in the latter pastes. As the XRPD and FTIR data showed, the 28 days, 4 M NaOH-activated

pastes had a high calcite content, a result of the interaction between atmospheric CO_2 and the calcium ions in the material. Inasmuch as these pastes had no portlandite, the calcium was necessarily sourced from the C-S-H/C-A-S-H gel initially formed [46].

The mechanisms governing alkali-activated materials are presently under study by a number of authors, for many factors are involved, including type of starting materials [51], activator type [47], relative humidity [52] and CO_2 concentration [53]. The reasons underlying the higher carbonation in the 4 M than in the 6 M or 8 M NaOH-activated pastes are fairly complex. Bernal et al. [54] observed the carbonation rate to decline with rising activator concentration in calcium-high alkali-activated systems (such as metakaolin + slag) due to the more intense carbonate salt precipitation generated by the interaction between the highly alkaline solution and the CO_2 in the air. Carbonate salt precipitation would lower the pore volume in the matrix, hindering additional CO_2 ingress in the sample and carbonation progression [54]. As noted earlier, further to the XRD and SEM data, the 6 and 8 M NaOH-activated pastes, rather than developing high calcite contents, precipitated sodium and sodium-calcium carbonates such as natron and para-alumohydrocalcite/hemicarboaluminate.

Briefly, the rise in the degree of reaction with higher activator concentration, proven by the appearance of progressively more compact matrices in the pastes studied (Figure 5), would explain the higher compressive strength values in the 6 and 8 M than in the 4 M NaOH-activated pastes. The higher two and 28 days strength in the pastes studied here, than by other authors, was associated with a higher degree of reaction over time and the formation of gels with greater silicon and calcium contents.

There are different factors that affect the development of mechanical strength such as: total porosity, size and porous distribution, degree of reaction, type and morphology of the reaction product, structure and composition of cementitious gels, etc. All these aspects are important and depend on the reactivity of the precursor and the alkaline solution used and the curing procedure. In the literature, there are already works that use molecular dynamics simulations to evaluate the fracture toughness of C-S-H [55] techniques. In this work, we have focused on the chemical aspects (instead of the physical characteristics). In addition, the high SiO_2/Al_2O_3 ratio and the co-precipitation of C-A-S-H and (N,C)-A-S-H gels observed in all the pastes studied might explain the high strength of our materials (higher than the ones reported for studies using common low-calcium clays) [5,22–25].

4. Conclusions

The most prominent conclusions to be drawn from this study are listed below.

- NaOH (at concentrations of 4, 6 and 8 M) activation of a carbonate-high illite clay contributes to paste hardening at ambient temperature. The presence of reactive calcium in the starting clay induces co-precipitation of a mix of gels: an aluminium-enriched C-S-H gel (C-A-S-H) and a N-A-S-H gel, in which sodium is partially replaced by calcium (N,C)-A-S-H.
- When the activator is a 4 M NaOH solution, the C-A-S-H gel is more intensely carbonated than with 6 or 8 M activators.
- Pastes prepared with higher (6 or 8 M) activator concentrations exhibit a more compact matrix than the ones prepared with 4 M NaOH. Given the comparability of the findings for the 6 and 8 M NaOH-activated pastes and the cost effectiveness of using a lower concentration activator, the 6 M NaOH solution may be deemed to be the most suitable of those studied here. Activating a mechanically and thermally pre-treated carbonate-high illite clay with a 6 M NaOH solution can deliver a binder with two days compressive strength of >20 MPa and 28 days strength of >30 MPa.

Author Contributions: A.D., Formal analysis; writing—original draft. D.P. and A.F.-J., Methodology; Investigation; Supervision; Resources; Writing—review & editing; Funding acquisition. G.E., R.L. and A.P., Writing—review & editing. All authors have read and agreed to the published version of the manuscript.

Funding: The research was also partially funded by the Spanish Ministry of the Economy, Industry and Competitiveness and ERDF under project BIA2016-76466-R.

Acknowledgments: The authors gratefully acknowledge the Italian Ministry of Education, University and Research (MIUR Funds—PhD in Geosciences, University of Bari) and the University of Bari for ordinary financial support (ex 60% Founds).

Conflicts of Interest: The authors declare no conflict of interest.

References

1. Xu, H.; van Deventer, J. The geopolymerisation of alumino-silicate minerals. *Int. J. Miner. Process.* **2000**, *59*, 247–266. [CrossRef]
2. Alonso, S.; Palomo, A. Alkaline activation of metakaolin and calcium hydroxide mixtures: Influence of temperature, activator concentration and solids ratio. *Mater. Lett.* **2001**, *47*, 55–62. [CrossRef]
3. Granizo, M.L.; Alonso, S.; Blanco-Varela, M.T.; Palomo, A. Alkaline Activation of Metakaolin: Effect of Calcium Hydroxide in the Products of Reaction. *J. Am. Ceram. Soc.* **2002**, *85*, 225–231. [CrossRef]
4. Fernández-Jiménez, A.; Monzo, M.; Vincent, M.B.A.; Palomo, A. Alkaline activation of metakaolin-fly ash mixtures: Obtain of Zeoceramics and Zeocements. *Microporous Mesoporous Mater.* **2008**, *108*, 41–49. [CrossRef]
5. Ferone, C.; Colangelo, F.; Cioffi, R.; Montagnaro, F.; Santoro, L. Use of reservoir clay sediments as raw materials for geopolymer binders. *Adv. Appl. Ceram.* **2013**, *112*, 184–189. [CrossRef]
6. Davidovits, J. Geopolymers: Inorganic Polymeric New Materials. *J. Therm. Anal.* **1991**, *37*, 1633–1656. [CrossRef]
7. Scrivener, K.; Martirena, F.; Bishnoi, S.; Maity, S. Calcined clay limestone cements (LC3). *Cem. Concr. Res.* **2018**, *114*, 49–56. [CrossRef]
8. Dhandapani, Y.; Sakthivel, T.; Santhanam, M.; Gettu, R. Pillai Mechanical properties and durability performance of concretes with limestone calcined clay cement (LC^3). *Cem. Concr. Res.* **2018**, *107*, 136–151. [CrossRef]
9. Scrivener, K.L.; John, V.M.; Gartner, E.M. Eco-efficient cements: Potential economically viable solutions for a low-CO_2 cement-based materials industry. *Cem. Concr. Res.* **2018**, *114*, 2–26. [CrossRef]
10. Alvarez-Pinazo, G.; Santacruz, I.; Aranda, M.A.; De la Torre, A.G. Hydration of belite–ye'elimite–ferrite cements with different calcium sulfate sources. *Adv. Cem. Res.* **2016**, *28*, 1–15. [CrossRef]
11. Palomo, A.; Krivenko, P.; García-Lodeiro, I.; Kavalerova, E.; Maltseva, O.; Fernández-Jiménez, A. A review on alkaline activation: New analytical perspectives. *Materiales Construcción* **2014**, *64*, e022. [CrossRef]
12. Provis, J.L.; van Deventer, J.S.J. (Eds.) *Alkali-Activated Materials: State-of-the-Art Report, RILEM TC 224-AAM*; Springer: Dordrecht, The Netherlands, 2014.
13. Provis, J.L. Alkali-activated materials. *Cem. Concr. Res.* **2018**, *114*, 40–48. [CrossRef]
14. Zhang, Z.H.; Zhu, H.J.; Zhou, C.H.; Wang, H. Geopolymer from kaolin in China: An overview. *Appl. Clay Sci.* **2016**, *119*, 31–41. [CrossRef]
15. Kuenzel, C.; Vandeperre, L.J.; Donatello, S.; Boccaccini, A.R.; Cheeseman, C. Ambient Temperature Drying Shrinkage and Cracking in Metakaolin-Based Geopolymers. *J. Am. Ceram. Soc.* **2012**, *95*, 3270–3277. [CrossRef]
16. Liew, Y.-M.; Heah, C.-Y.; Mustafa, A.B.M.; Kamarudin, H. Structure and properties of clay-based geopolymer cements: A review. *Prog. Mater. Sci.* **2016**, *83*, 595–629. [CrossRef]
17. Brigatti, M.F.; Galán, E.; Theng, B.K.G. Structure and Mineralogy of Clay Minerals. In *Handbook of Clay Science*; Bergaya, F., Lagaly, G., Eds.; Elsevier: Oxford, UK, 2013; pp. 21–81.1148. [CrossRef]
18. Murray, H.H. *Applied Clay Mineralogy: Occurrences, Processing and Application of Kaolins, Bentonites, Palygorskite-Sepiolite, and Common Clays*; Elsevier: Amsterdam, The Netherlands, 2006.
19. Seiffarth, T.; Hohmann, M.; Posern, K.; Kaps, C. Effect of thermal pre-treatment conditions of common clays on the performance of clay-based geopolymeric binders. *Appl. Clay Sci.* **2013**, *7*, 35–41. [CrossRef]
20. Ferone, C.; Liguori, B.; Capasso, I.; Colangelo, F.; Cioffi, R.; Cappelletto, E.; di Maggio, R. Thermally treated clay sediments as geopolymer source material. *Appl. Clay Sci.* **2015**, *107*, 195–204. [CrossRef]
21. D'Elia, A.; Pinto, D.; Eramo, G.; Giannossa, L.C.; Ventruti, G.; Laviano, R. Effects of processing on the mineralogy and solubility of carbonate-rich clays for alkaline activation purpose: Mechanical, thermal activation in red/ox atmosphere and their combination. *Appl. Clay Sci.* **2018**, *152*, 9–21. [CrossRef]

22. Duxson, P.; Lukey, G.C.; van Deventer, J.S.J. Physical evolution of Na-geopolymer derived from metakaolin up to 1000 °C. *J. Mater. Sci.* **2007**, *42*, 3044–3054. [CrossRef]
23. Granizo, M.L.; Blanco-Varela, M.T.; Palomo, A. Influence of the starting kaolin on alkali-activated materials based on metakaolin. Study of the reaction parameters by isothermal conduction calorimetry. *J. Mater. Sci.* **2000**, *35*, 6309–6315. [CrossRef]
24. Palomo, A.; Blanco-Varela, M.T.; Granizo, M.L.; Puertas, F.; Vazquez, T.; Grutzeck, M.W. Chemical stability of cementitious materials based on metakaolin. *Cem. Concr. Res.* **1999**, *29*, 997–1004. [CrossRef]
25. Buchwald, A.; Hohmann, M.; Posern, K.; Brendler, E. The suitability of thermally activated illite/smectite clay as raw material for geopolymer binders. *Appl. Clay Sci.* **2009**, *46*, 300–304. [CrossRef]
26. Essaidi, N.; Samet, B.; Baklouti, S.; Rossignol, S. Effect of calcination temperature of Tunisian clay on the properties of geopolymers. *Ceramics Silikáty* **2013**, *57*, 251–257.
27. Ruiz-Santaquiteria, C.; Fernández-Jiménez, A.; Skibsted, J.; Palomo, A. Clay reactivity: Production of alkali activated cements. *Appl. Clay Sci.* **2013**, *73*, 11–16. [CrossRef]
28. García-Lodeiro, I.; Cherfa, N.; Zibouche, F.; Fernández-Jimenez, A.; Palomo, A. The role of aluminium in alkali-activated bentonites. *Mater. Struct.* **2015**, *48*, 585–597. [CrossRef]
29. Garcia-Lodeiro, A.; Fernandez-Jimenez, A. Palomo Hybrid Alkaline Cements: Bentonite-Opc Binders. *Minerals* **2018**, *8*, 137. [CrossRef]
30. Khater, H.M. Effect of Calcium on Geopolymerization of Aluminosilicate Wastes. *J. Mater. Civ. Eng.* **2012**, *24*, 92–101. [CrossRef]
31. Temuujin, J.; van Riessen, A.; Williams, R. Influence of calcium compounds on the mechanical properties of fly ash geopolymer pastes. *J. Hazard. Mater.* **2009**, *167*, 82–88. [CrossRef]
32. García-Lodeiro, I.; Palomo, A.; Fernández-Jiménez, A.; Macphee, D. Compatibility studies between N-A-S-H and C-A-S-H gels. Study in the ternary diagram Na_2O-CaO-Al_2O_3-SiO_2-H_2O. *Cem. Concr. Res.* **2011**, *41*, 923–931. [CrossRef]
33. Alahrache, S.; Winnefeld, F.; Champenois, J.B.; Hesselbarth, F.; Lothenbach, B. Chemical activation of hybrid binders based on siliceous fly ash and Portland cement. *Cem. Concr. Compos.* **2006**, *66*, 10–23. [CrossRef]
34. García-Lodeiro, I.; Donatello, S.; Fernández-Jiménez, A.; Palomo, A. Hydration of Hybrid Alkaline Cement Containing a Very Large Proportion of Fly Ash: A Descriptive Model. *Materials* **2016**, *9*, 605. [CrossRef] [PubMed]
35. Moore, D.M.; Reynolds, R.C., Jr. *X-ray Diffraction and the Identification and Analysis of Clay Minerals*, 2nd ed.; Oxford University Press: New York, NY, USA, 1997.
36. Komljenović, M.; Bascarević, Z.; Bradić, V. Mechanical and microstructural properties of alkali-activated fly ash geopolymers. *J. Hazard. Mater.* **2010**, *181*, 35–42. [CrossRef]
37. Criado, M.; Palomo, A.; Fernández-Jiménez, A. Alkali activation of fly ashes. Part 1: Effect of curing conditions on the carbonation of the reaction products. *Fuel* **2005**, *84*, 2048–2054. [CrossRef]
38. Myers, R.J.; Bernal, S.A.; Provis, J.L. Phase diagrams for alkali-activated slag binders. *Cem. Concr. Res.* **2017**, *95*, 30–38. [CrossRef]
39. Cwirzen, A.; Provis, J.L.; Penttala, V.; Habermehl-Cwirzen, K. The effect of limestone on sodium hydroxide-activated metakaolin-based geopolymers. *Constr. Build. Mater.* **2014**, *66*, 53–62. [CrossRef]
40. Rees, C.; Provis, J.L.; Luckey, G.C.; van Deventer, J.S.J. In Situ ATR-FTIR Study of the Early Stages of Fly Ash Geopolymer Gel Formation. *Langmuir* **2007**, *23*, 9076–9082. [CrossRef] [PubMed]
41. Criado, M.; Fernández-Jiménez, A.; Palomo, A. Alkali activation of fly ash: Effect of the SiO_2/Na_2O ratio Part I: FTIR study. *Microporous Mesoporous Mater.* **2007**, *106*, 180–191. [CrossRef]
42. Yu, P.; Kirkpatrick, R.J.; Poe, B.; McMillan, P.F.; Cong, X. Structure of Calcium Silicate Hydrate (C-S-H): Near-, Mid-, and Far-Infrared Spectroscopy. *J. Am. Ceram. Soc.* **1999**, *82*, 742–748. [CrossRef]
43. Joshi, S.; Kalyanasundaram, S.; Balasubramanian, V. Quantitative Analysis of Sodium Carbonate and Sodium Bicarbonate in Solid Mixtures Using Fourier Transform Infrared Spectroscopy (FT-IR). *Appl. Spectrosc.* **2013**, *67*, 841–845. [CrossRef]
44. Yip, C.; Lukey, G.; Provis, J.; van Deventer, J. Effect of calcium silicate sources on geopolymerisation. *Cem. Concr. Res.* **2008**, *38*, 554–564. [CrossRef]
45. Yip, C.; Provis, J.; Lukey, G.; van Deventer, J. Carbonate mineral addition to metakaolin-based geopolymers. *Cem. Concr. Compos.* **2008**, *30*, 979–985. [CrossRef]

46. Puertas, F.; Palacios, M.; Vazquez, T. Carbonation process of alkali-activated slag mortars. *J. Mater. Sci.* **2006**, *41*, 3071–3082. [CrossRef]
47. Puertas, F.; Palacios, M.; Manzano, H.; Dolado, J.S.; Rico, A.; Rodríguez, J. A model for the C-A-S-H gel formed in alkali-activated slag cements. *J. Eur. Ceram. Soc.* **2011**, *31*, 2043–2056. [CrossRef]
48. Fernández-Jiménez, A.; Zibouche, F.; Boudissa, N.; García-Lodeiro, I.; Abadlia, M.T.; Palomo, A. Metakaolin-Slag-Clinker Blends. The role of Na^+ or K^+ as Alkaline Activators of Theses Ternary Blends. *J. Am. Ceram. Soc.* **2013**, *96*, 1–8. [CrossRef]
49. García-Lodeiro, I.; Fernández-Jiménez, A.; Palomo, A. Hydration kinetics in hybrid binders: Early reaction stages. *Cem. Concr. Compos.* **2013**, *39*, 82–92. [CrossRef]
50. Liu, B.; Ray, A.S.; Thomas, P.S. Strength development in autoclaved aluminosilicate rich industrial waste cement systems containing reactive magnesia. *J. Aust. Ceram. Soc.* **2007**, *43*, 82–87.
51. Bernal, S.A.; Provis, J.L.; Walkley, B.; Nicolas, R.S.; Gehman, J.D.; Brice, D.G.; Kilcullen, A.; Duxson, P.; van Deventer, J.S.J. Gel nanostructure in alkali-activated binders based on slag and fly ash, and effects of accelerated carbonation. *Cem. Concr. Res.* **2013**, *53*, 127–144. [CrossRef]
52. Bernal, S.A.; Provis, J.L.; de Gutiérrez, R.M.; van Deventer, J.S.J. Accelerated carbonation testing of alkali-activated slag/metakaolin blended concretes: Effect of exposure conditions. *Mater. Struct.* **2015**, *48*, 653–669. [CrossRef]
53. Bernal, S.A.; Provis, J.L.; Brice, D.G.; Kilcullen, A.; Duxson, P.; van Deventer, J.S.J. Accelerated carbonation testing of alkali-activated binders significantly underestimate the real service life: The role of the pore solution. *Cem. Concr. Res.* **2012**, *42*, 1317–1326. [CrossRef]
54. Bernal, S.A. Effect of the activator dose on the compressive strength and accelerated carbonation resistance of alkali silicate-activated slag/metakaolin blended materials. *Constr. Build. Mater.* **2015**, *98*, 217–226. [CrossRef]
55. Bauchy, M.; Laubie, H.; Qomi, M.A.; Hoover, C.G.; Ulm, F.J.; Pellenq, R.M. Fracture toughness of calcium–silicate–hydrate from molecular dynamics simulations. *J. Non-Cryst. Solids* **2015**, *419*, 58–64. [CrossRef]